# Distributed cooperative energy management system of connected hybrid electric vehicles with personalized non-stationary inference

Li, Ji; Zhou, Quan; He, Yinglong; Williams, Huw; Xu, Hongming; Lu, Guoxiang

[Link to publication on Research at Birmingham portal](#)

# Distributed Cooperative Energy Management System of Connected Hybrid Electric Vehicles with Personalized Non-Stationary Inference

Ji Li, *Member, IEEE*, Quan Zhou, *Member, IEEE*, Yinglong He, Huw Williams, Hongming Xu, and Guoxiang Lu

*Abstract*—This paper develops a distributed cooperative energy management system with two distributed control layers for speed-coupling plug-in hybrid electric vehicles. By introducing personalized non-stationary inference, this system can fuse driving behavior and vehicle state information to adaptively adjust power-split control parameters for the improvement of vehicle energy economy. In the on-board control layer, five sets of personalized control parameters are optimized offline by using chaos-enhanced accelerated particle swarm optimization. In the distributed control layer, interval type-2 fuzzy sets are applied to develop a real-time driving style recognition function. Driving behavior is detected remotely, via the vehicle to everything network, and downloaded to adaptively adjust power-split control parameters in the on-board vehicle controller. Hardware-in-the-loop testing is carried out based on the four laboratory driving cycles and four personal driving cycles. The proposed system has been demonstrated with strong robustness that saves energy by up to 5.25% over the equivalent consumption minimization strategy (ECMS), especially for gentle drivers. Even under harsh communication conditions (with signal loss 80+%), it still performs better than the ECMS (by 0.57%) and the series-parallel control strategy (by 2.66%).

*Index Terms*—Connected hybrid electric vehicle; distributed decision-making; energy management personalization; interval type-2 fuzzy logic set; non-stationary inference

### ABBREVIATION

| | |
|---|---|
| ECMS | Equivalent consumption minimization strategy |
| PHEV | Plug-in hybrid electric vehicles |
| EMS | Energy management system |
| CD | Charge depleting |
| CS | Charge sustaining |
| FLC | Fuzzy logic controller |
| V2X | Vehicle to everything |
| V2I | Vehicle-to-infrastructure |
| SP | Series-parallel |
| ICE | Internal combustion engine |
| ISG | Integrated starter-generator |
| SoC | State of charge |
| CAPSO | Chaos-enhanced accelerated particle swarm optimization |
| IT2 | Interval type 2 |
| APSO | Accelerated particle swarm optimization |

### NOMENCLATURE

| | |
|---|---|
| $M$ | Gross mass |
| $A_f$ | Windward area |
| $R_{wh}$ | Tire rolling radius |
| $C_d$ | Air drag coefficient |
| $i_0$ | Differential ratio |
| $i_g$ | Transmission ratio |
| $T_d$ | Torque demand |
| $n_d$ | Speed demand |
| $g$ | Gravitational constant |
| $\delta$ | Coefficient of rolling friction |
| $u_a$ | Vehicle speed |
| $\theta$ | Slope grade |
| $\xi$ | Power-split vector |
| $T_{mot}$ | Trans-motor torque |
| $n_{mot}$ | Trans-motor rotation speed |
| $T_{ice}$ | Engine torque |
| $n_{ice}$ | Engine rotation speed |
| $P_{gen}$ | Integrated starter-generator power |
| $\chi$ | Proportionality factor |
| $SoC$ | State of charge |
| $\delta$ | Degree of accelerator pedal depression |
| $e$ | Error of tracking speed |
| $\lambda$ | Style factor |
| $E_{fuel}$ | Instantaneous fuel consumption |
| $\omega_l$ | Firing strength of rule $l$ |
| $\mu_{F_i^l}$ | Membership grades |
| $\widetilde{K}_r$ | $r$th local linear control gain |
| $u$ | Crisp output |
| $\phi$ | Control parameter of power-split rules |

## I. INTRODUCTION

ELETRIC vehicles, including battery electric vehicles, plug-in hybrid electric vehicles (PHEVs), and fuel cell electric vehicles are the main contributors towards net zero emissions in the transport sector [1]. To bridge the transition to battery electric and other renewable vehicles, hybrids and plug-in hybrids play an essential role in prior technical experience and market expansion [2]. The design of the energy management system (EMS) for PHEVs is critical to minimizing energy consumption and exhaust emissions, and it is a challenging task that needs to deal with the uncertainty and the complexity of driving conditions [3].

Heuristic supervisory control systems have been favored by industry due to easy implementation and strong robustness [4]. These rules are designed based on human expertise and/or mathematical models, and there is usually no prior driving information [5]. In automotive industry, charge depleting (CD) and charge sustaining (CS) strategy is widely used for PHEVs due to its explicit mode definition [6]. There is a challenging

Ji Li, Quan Zhou, Yinglong He, Huw Williams, and Hongming Xu are with the Department of Mechanical Engineering, the University of Birmingham, Birmingham B15 2TT, U.K. (e-mail: j.li.1@bham.ac.uk; q.zhou@pgr.bham.ac.uk; yxh701@bham.ac.uk; h.williams.5@bham.ac.uk; h.m.xu@bham.ac.uk). Guoxiang Lu is with Shenzhen BYD Auto Co Ltd, Guangzhou City, China (e-mail: lu.guoxiang@byd.com).

task to define mode switching conditions and their performance is mainly determined by expert knowledge and driving scenario choice. To reduce the development workload for energy management controllers, Quan et al. research a transferable representation modelling routine, where two artificial intelligence technologies of deep neural network [7] and Gaussian process regression [8] are developed to cooperate with an adaptive neuro-fuzzy inference system for knowledge transfer of the energy management controller. The equivalent consumption minimizing strategy (ECMS) [9] is an online method to transform a global minimization problem into an instantaneous minimization problem that must be solved at each time step. The equivalent factor can be evaluated on the basis of past and predicted data of the driving conditions [10]. Dynamic programming [11] is able to effectively deal with the nonlinearity and constraints of problems e.g. PHEV energy management. Its optimal results can be used to adapt to similar driving conditions by re-calibration into fixed rules [12] or neural networks [13]. However, their limitations remain obvious due to computational burden and the poor adaptability of the control system to various driving styles.

As the primary decision-maker of modern vehicles, human driver plays an important role in driving safety as well as in eco-driving. Therefore, a vehicle control strategy that seeks a highly optimized performance which requires optimizing the system composed of the vehicle and the driver, needs to explicitly consider driver behavior [14]. For the classification of driving events, driving style can be grouped according to the fuel already contained or the total energy consumption [15], [16]. The use of the rule base algorithm unifies simplicity, is easy to explain and implement, but limits the number of parameters that can be managed. Larger sets of variables generate unnecessarily complex rules that can be substituted by fuzzy logic maps. Syed et al. proposed an fuzzy logic algorithm to evaluate optimal operation of the pedals in HEVs [17]. The algorithm can monitor the operation of the gas pedal and brake pedal, and then can calculate the appropriate correction value and produce tactile feedback to the driver. Unsupervised algorithms do not need to understand the underlying process. In the work of Miyajima et al., a Gaussian mixture model was implemented based on the analysis of car-following behavior and pedal operation spectrum [18]. However, the output needs to be guided based on the number of interpretations and clusters.

Distributed control provides advantages in terms of faster computation, and less communication, and increased modularity [19]. For future connected and automated vehicles, distributed control could also have security advantages, allowing coordination between networked storage systems without data centralization, which could lead to intellectual property and privacy concerns [20]. Assisted by edge and cloud computing services, it is possible to reduce computational burden of an on-broad vehicle controller and apply complex algorithms for restricting the vehicles' real-world emissions via inter-vehicle communication [21]. Duan et al. present a distributed cloud fog computing architecture for energy management of smart grids considering the high penetration of PHEVs [22], where this distributed framework let neighboring

agents to get into a consensus with each other. With help of Grey Wolf Optimizer, the simulation result shows the appropriate efficiency of this layout. Li et al. and Hu et al. demonstrated that adaptive modelling can be achieved through vehicle to everything (V2X) data and connected computing resources [23], [24]. In the Lin et al., a software defined Internet of Vehicles architecture based on edge intelligence distributed learning is established for supporting real-time vehicle routing decision via distributed multi-agent reinforcement learning models [25]. By numerical study, this scheme has an ability to alleviate traffic congestion with the dynamic changes of the road environment. However, as Li et al. pointed out in [26], communication issues, such as time delays, quantization errors, and packet loss pose a significant challenge to vehicle distributed control. Up to now, few noticeable works have been documented within the context of EMSs of connected vehicles considering communication issues.

It is clear from the literature study above, the development of next generation of PHEV EMSs needs to overcome the following existing technical barriers: 1) driving behaviors cannot be captured and utilized well in the onboard EMSs due to limits of computation resources; 2) design of heuristic rules for EMSs is dependent on human expertise and has poor adaptability to various driving styles; and 3) for distributed EMSs, communication issues happen from time to time but the treatment for signal losses and delays is rarely considered in the literature. To systematically address the identified technical challenges, this paper develops a distributed cooperative energy management system for connected PHEVs that incorporates the factor of driving styles into the vehicle control optimization. Based on the authors' recent research in optimization of hybrid powertrain systems in distributed decision making [27] and fusion of driver-related information [28], a new approach of using personalized non-stationary inference is introduced to increase adaptability of the EMS to various driving styles.

This paper is organized as follows: after the introduction, a connected PHEV with its EMS is analyzed in section II. The mechanism of the proposed distributed cooperative EMS is described in section III, which involves two principal parts of inference rule personalization and driving style recognition. Section IV sets out the testing cycle and the HiL experimental platform that was used. Section V discusses the results of: the energy-saving performance; the vehicle system performance; and the communication efficiency comparison. Conclusions are summarized in section VI.

## II. Connected Hybrid Electric Vehicles

Modern road traffic is a complicated and interconnected system, which incorporates traffic information centers, monitoring infrastructure, and vehicles with diverse energy sources. The V2X network is the communication medium of intelligent transport systems, connecting vehicles, infrastructure and information centers, wherein dedicated short-range communication (DSRC) and 4G-LTE are two widely used candidate protocols. V2X possesses powerful cloud computing facilities that can implement an advanced optimization scheme for connected vehicles. This system has

great potential to save energy for each connected vehicle and even for the whole transport system by managing traffic and individual vehicle operation.
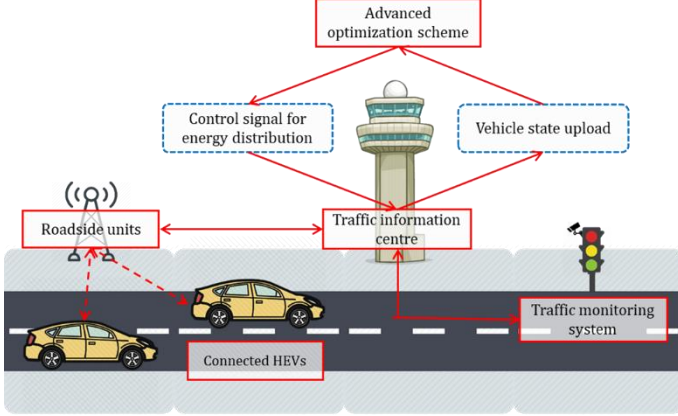


Fig. 1. The connected vehicle communication framework

Fig. 1 shows the connected vehicle communication scenario studied in this paper, and the workflow is as follows: 1) roadside units receive the PHEV real-time state signal through the vehicle-to-infrastructure (V2I) network (data throughput for a single connected vehicle at 60 km/h: DSRC: 27Mbps; 4G-LTE: 4Mbps [29]); 2) the information center collects the PHEV real-time state signal from the roadside units and operates an advanced optimization scheme to determine optimal control signals; and 3) the information center refers the control signal to the vehicle controller via the roadside units. This framework with cyber-physical technology can implement advanced intelligent algorithms to enable real-time driver-oriented energy management, which was formerly restricted by the performance of isolated vehicle controllers. As an increase of connected vehicles and their speeds, however, signal delay or loss of using either DSRC or 4G-LTE will come out as reported in [30] that needs be carefully concerned in the design of distributed EMSs.

*A. PHEV Configuration*

As illustrated in Fig. 2(a), the PHEV has a series-parallel (SP) topology, which comprises a 63kW internal combustion engine (ICE), a 32kW integrated starter-generator (ISG), and a 75kW trans-motor with (i.e., an electric motor that has a float stator [31]), where their state-steady efficiency maps are validated by Argonne National Laboratory. The main parameters for vehicle modelling are illustrated in Table I. They were sourced from the authors' recent work [32] and are representative of a typical family car, where a 2RC electrical model [33] has been adopted to formulate a battery pack which consists of the battery cell type NCR-18650 series supplied by Panasonic Automotive & Industrial System Ltd.

TABLE I
MAIN PARAMETERS OF THE PHEV MODEL

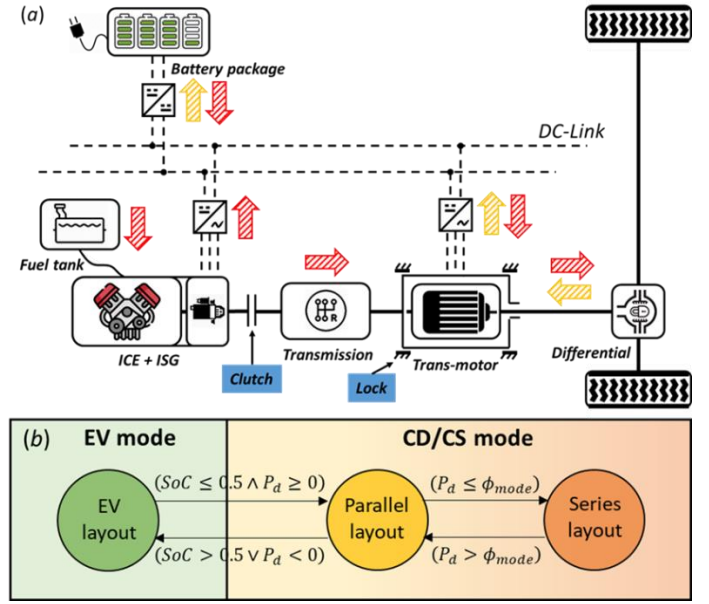| Symbol | Parameters | Values |
|--------|-----------|--------|
| $M$ | Gross mass | 1,500 kg |
| $A_f$ | Windward area | 2 m² |
| $R_{wh}$ | Tire rolling radius | 0.3 m |
| $C_d$ | Air drag coefficient | 0.3 |
| $i_0$ | Differential ratio | 3.75 |
| $i_g$ | Transmission ratio | 3.55/1.96/1.30/0.89/0.71 |



Fig. 2. The studied series-parallel PHEV: a) architecture of hybrid powertrain; and b) control strategy

By controlling the disengagement/engagement of the clutch and lock, the PHEV can work on three operational modes, i.e., EV mode, parallel mode, and series mode. If the clutch is disengaged, and Lock is engaged, the PHEV will work at the EV mode like an electric vehicle. If the clutch is engaged, and Lock is disengaged, the PHEV will work at the parallel mode where the engine is used for propulsion. If the clutch is disengaged, and lock is engaged, the PHEV will work at the series mode where the engine is used for charging the battery.

A backward facing vehicle model considering longitudinal dynamics is used in this study. The torque demand $T_d$ and rotation speed demand $n_d$ after a bi-level-gear speed reducer are:

$$\left. \begin{array}{c} T_d = \left( \delta ma + \dfrac{C_d A_f u^2}{21.15} + mg\sin\theta + mgf\cos\theta \right) \cdot \dfrac{R_{wh}}{i_0 \cdot \eta_{i0}} \\[3mm] n_d = 9.55 \cdot \dfrac{u_a}{3.6 \cdot R_{wh}} \end{array} \right\} (1)$$

where, $g = 9.81 m/s^2$ is gravitational constant; $\delta = 1$ is the coefficient of rolling friction; $u_a$ is the vehicle speed in km/h which is defined by driving cycles; $\theta = 0$ is slope grade; 9.55 is a conversion coefficient from radian per second to revolution per minute. For this model to be valid, we assume the PHEV has an available energy budget for a particular journey.

*B. Baseline Energy Management Strategy*

A typical SP control strategy [12] including electric traction mode (EV), charge depletion (CD) and charge sustaining (CS) modes is adopted in the on-board controller, as illustrated in Fig. 2(b), to ensure robustness and computational efficiency of the EMS. The inputs are vehicle torque demand, $T_d$, speed demand, $n_d$, and battery state of charge, $SoC$. It is used to determine a power-split vector $\boldsymbol{\xi}$ which is constructed in Eq. (2) from the trans-motor torque, $T_{mot}$; the trans-motor speed, $n_{mot}$; the ICE torque, $T_{ice}$; the ICE speed, $n_{ice}$; and the ISG power, $P_{gen}$.

$$\xi = [T_{mot} \quad n_{mot} \quad T_{ice} \quad n_{ice} \quad P_{gen}] \quad (2)$$

In the EV mode (when $SoC > 0.5$ or $P_d < 0$), electricity can be provided to satisfy power demand of the PHEV independently so that both the ICE and the ISG do not need to work. The power allocation under the EV mode is described as follows:

$$\xi = [T_d \quad n_d \quad 0 \quad 0 \quad 0] \quad (3)$$

In the CD/CS mode (when $SoC \leq 0.5$ and $P_d \geq 0$), a PHEV will normally favor electric traction, and then the battery will subsequently be charged through the power grid. If the battery pack's state of charge (SoC) falls below its target level, the ICE will be applied to charge the battery in a CS mode. In this state, the ECU will coordinate transition between series and parallel layouts to maximize the energy economy. A control parameter, $\phi_{mode}$ will introduced and calibrated in our recent study [32]. If $P_d > \phi_{mode}$, the vehicle will work on parallel layout otherwise the vehicle will work on series layout. The detailed power distribution is described as follows:

$$\xi = \begin{cases} [T_d \quad n_d \cdot (1-\chi_1) \quad T_d \quad n_d \cdot \chi_1 \quad 0] & Series \\ [T_d \quad n_d \quad T'_{ice}(P_{gen}) \quad n'_{ice}(P_{gen}) \quad P_{gen^+} \cdot \chi_2] & Parallel \end{cases} \quad (4)$$

where, $T'_{ice}$ and $n'_{ice}$ are optimal torque and speed of the ICE converted based on demand power of the ISG $P_{gen}$; $P_{gen}^+$ is the maximum power of the ISG; $\chi_i$ ($i$=1 or 2) is a proportionality factor determined by SoC as follows, $\chi_1$ and $\chi_2$ are for ICE control and ISG control, respectively [34].

$$\chi_i(SoC)$$
$$= \begin{cases} 1, & SoC \in [0,0.2] \\ \dfrac{1}{1 + \exp\left\{\left(\dfrac{SoC}{SoC^*} + \phi_\beta\right)\phi_\alpha\right\}}, & SoC \in (0.2,0.5] \\ 0, & SoC \in (0.5,0.8] \end{cases} \quad (5)$$

where, $SoC^*$ is a scaling coefficient of the BP's SoC; and $\phi_{i,\alpha}$ ($i$=1 or 2) $\in [0.01,50]$ and $\phi_{i,\beta}$ ($i$=1 or 2) $\in [-6,6]$ are four control parameters introduced here to enable optimization of cut-in timing and conversion speed of the ICE and ISG. They separately define the position and slope of the curve in the logistic function.

## III. DISTRIBUTED COOPERATIVE ENERGY MANAGEMENT SYSTEM

In order to improve adaptability of the EMS to various driving behaviors, the distributed cooperative EMS with two distributed control layers is developed and presented in Fig. 3. This EMS allows the fusion of driving behavior and vehicle state information to adaptively adjust power-split control parameters. In the on-board control layer, the chaos-enhanced accelerated particle swarm optimization (CAPSO) algorithm is implemented to offline optimize control parameters of the SP strategy based on the classified driving styles. In the distributed control layer, a real-time driving style recognition function using interval type-2 (IT2) fuzzy sets is developed to identify driving styles. The proposed EMS is expected to subvert the traditional reasoning process by activating its stationary inference. Via the V2X network, the distributed server receives uploaded feedback information, analyses driving behavior, and computes real-time control signals. Those signals will be downloaded to adjust the control parameters for minimizing the energy consumption and to maintain the SoC.
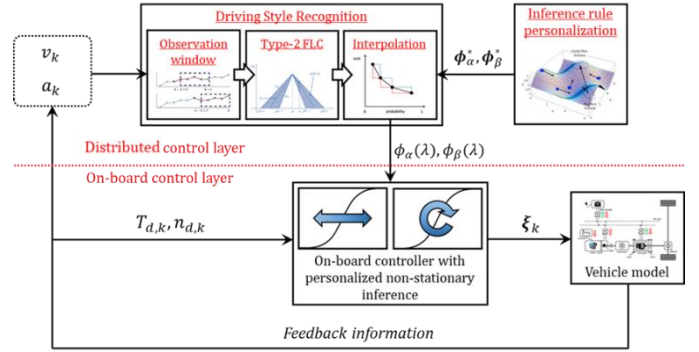


Fig. 3. The framework of the proposed distributed cooperative EMS

### A. Inference Rule Personalization

Before being able to adaptively adjust control parameters of the SP strategy, the control parameters need to be well defined. Inference rule personalization aims to tailor independent control parameters of the SP strategy for different driving behaviors. The design procedure of the inference rule personalization can be divided into three main steps: 1) driver-oriented cycle reproduction; 2) problem formulation; and 3) CAPSO implementation.

In the driver-oriented cycle reproduction, the approach of processing the accelerator pedal's angle of depression is commonly used for driving style classification. Zhang et al. provide a simplified sub-model to describe different types of driving style by adjusting a style factor $\lambda$ [35] and it is used here. Through the model, driving cycles with different driving styles can be assigned to five grades, Very Gentle, Gentle, Normal, Aggressive, and Very Aggressive. The driver sub-model is drawn as follows:
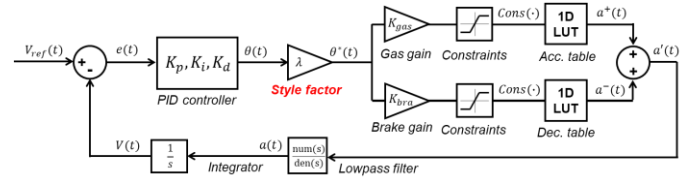


Fig. 4. The schematic diagram of the used driver sub-model

where, the style factor $\lambda \in [0,1]$ is an impact factor derived from the driving style type; the function $PID$ is a proportional–integral–derivative controller; $K_p, K_i, K_d$ are coefficients of proportional, integral and derivative terms, respectively; and $e_k$ is the error between the target speed, $v_{ref}$, and the vehicle speed, $v_k$. Through different settings of style factor, new degrees of gas and brake pedal depression with different driving styles can be obtained that is used to generate new driving profiles from the target speed, $v_{ref}$.

This paper studies a bi-objective optimization problem in PHEV energy management. The first optimization objective is to minimize the total energy consumption in fuel and electricity, $J_1$. The second optimization objective is to maximize the value of the remaining battery SoC at the end of a given driving cycle, $J_2$. They are given by

$$\left.\begin{array}{l} J_1 = \sum_{k=0}^{k=k_{end}} \left(E_{fuel} + E_{bp}\right) \\ J_2 = \dfrac{1}{SoC_{end}} \end{array}\right\} \quad (7)$$

where, $E_{fuel}$ is the instantaneous energy consumption from the fuel tank; $E_{bp}$ is the instantaneous energy consumption from the battery pack; and $SoC_{end}$ is the value of remaining battery SoC at the end of a given driving cycle. In the present work, the multi-objective optimization is formulated by using the weighted sum method.

Consequently, the energy-flow control optimization problem with constraints is expressed by

$$\begin{bmatrix} \phi_{1,\alpha}^* & \phi_{1,\beta}^* & \phi_{2,\alpha}^* & \phi_{2,\beta}^* \end{bmatrix} = \arg\min(J_1 \quad J_2) \qquad (8)$$
$$s.t. \begin{cases} \phi_\alpha^*, & \phi_\alpha \in \mathcal{A} \\ \phi_\beta^*, & \phi_\beta \in \mathcal{B} \end{cases}$$

For the given case study, the range of the control parameter $\phi_\alpha$ is between $\varepsilon_\alpha^- = 0.01$ and $\varepsilon_\alpha^+ = 50$, its limits are the lowest requirement to ensure a close to 0-90 degree slope search area (this also depends on the length of sampling time); the control parameter $\phi_\beta$ is constrained between $\varepsilon_\beta^- = -6$ and $\varepsilon_\beta^+ = 6$, and limited by its horizontal search range.
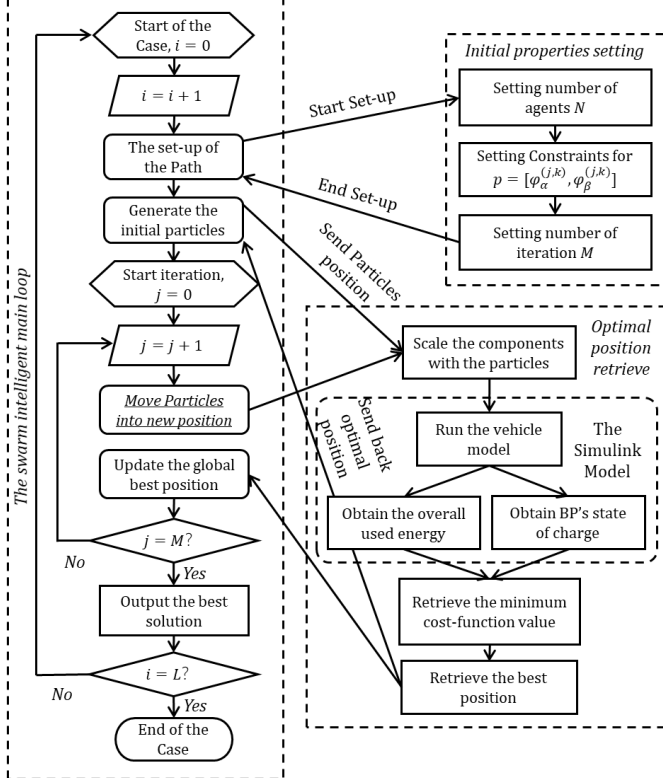


Fig. 5. The workflow of inference rule personalization by using CAPSO

The standard accelerated particle swarm optimization (APSO) always maintains the attraction factors as a static value [36]: In repetitive experiments, however, the solution is largely unchanged. Inspired by chaotic mapping strategy, the CAPSO algorithm [37] has a higher convergence speed and a greater probability of finding a global optimum. For personalizing the conventional stationary inference rule, this algorithm is tailored with an additional nest for different driving behaviors to obtain the optimal power-split control parameters over the driver-oriented WLTCs. As illustrated in Fig. 5, for each driving behavior $i$, the position of each particle is updated via:

$$x^{(j+1,k)} = (1-\delta)\, x^{(j,k)} + \delta\, g^{(j,*)} + \varepsilon^{(j)}\, r^{(j,k)} \qquad (9)$$

where, $g^{(j,*)}$ is the best position in the $j$th iteration; $\delta$ and $\varepsilon$ are the

attraction and convergence factors of CAPSO algorithm; and $r$ denotes a $U[0,1]$ random variable. Furthermore, $\varepsilon$ and $\delta$ obey the following equations to update for each iteration:

$$\left.\begin{aligned} \varepsilon^{(j)} &= \varepsilon^{(0)}\, \gamma^j, \\ \delta^{(j+1)} &= a\, \delta^{(j)}\, (1-\delta^{(j)}), \end{aligned}\right\} \qquad (10)$$

In Eq. (9), the settings, $\varepsilon^{(0)} = 0.9$ and $\gamma = 0.95$, are adopted; and the attraction factor is mapped by the logistic map, wherein the initial values $\delta^{(1)} = 0.6$ and $a = 4$ are applied. Once the index of driving behavior $i$ reaches the terminal condition $L = 5$, the program will end and then optimized control parameters will be recorded.

### B. Driving Style Recognition

To reduce computational burden on the onboard controller, driving style recognition is performed in the distributed control layer by the nonlinear model (recognizer) to monitor driving behavior, which includes an observation window, a type-2 FLC, and a final interpolation.

Firstly, a short-term sliding window is launched to restrict the sampling size and extend the residence time of recorded samples. Here, the dataset of speed and acceleration signals is established, where each time step k of data is described as follows:

$$(\boldsymbol{v}, \boldsymbol{a})^T = \begin{bmatrix} v_{k-h+1} & v_{k-h+2} & \cdots & v_k \\ a_{k-h+1} & a_{k-h+2} & \cdots & a_k \end{bmatrix} \qquad (11)$$

where, $\boldsymbol{v}$ is a vector of vehicle speed $(m/s)$; $\boldsymbol{a}$ is a vector of vehicle acceleration $(m/s^2)$; and $h = 60s$ is time width of the short-term sliding window. As the core of the reasoning mechanism, a type-2 FLC is used to differentiate driving style during real-time driving, which can be expressed mathematically as follows

$$\lambda = \text{FLC}(v_{avg}, a_{rng}) \qquad (12)$$

in which

$$\begin{cases} v_{avg} = \dfrac{\sum_{i=0}^{i=h}(\boldsymbol{v})^T}{h} \\ a_{rng} = \max(\boldsymbol{a})^T - \min(\boldsymbol{a})^T \end{cases} \qquad (13)$$

where, driving style $\lambda$ is a fuzzy logic function FLC of ranges of speed $v_{avg}$ and acceleration $a_{rng}$, and ranges of vehicle acceleration are assumed to reflect driving proficiency. In general, drivers with higher driving proficiency have a relatively low range. Average values of vehicle speed are adopted as considered in [38] to reflect driving habits.

Differing from type-1 fuzzy sets, type-2 fuzzy sets have the ability to handle higher-order uncertainty factors (e.g., driving behavior) at lower computational cost. In this case, type-2 fuzzy sets using linguistic terms are regulated by standard triangular membership functions (MFs), where the degree of membership is expressed as a function of normalized values in the interval, $[0,1]$. In order to manage a nonlinear plant based on the IT2 T–S fuzzy model as described in the work of Cao et al. [39], an IT2 T–S FLC is designed, and its fuzzy rules can be described as follows:

$R^{(r)}$: IF $z_1$ is $\tilde{F}_1^r$ and $z_2$ is $\tilde{F}_2^r$,..., and $z_v$ is $\tilde{F}_v^r$,

$\qquad$ THEN $u_k = \tilde{K}_r x_k$, $\qquad (r \in L \coloneqq 1,2,\dots,m)$

where $\tilde{K}_r$ denotes the $r$th local linear control gain. The output of this FLC is determined to be

$$u(k) = \sum_{r=1}^{m} f\left(\omega_r^L(x), \omega_r^U(x)\right) \widetilde{K}_r \, x \qquad (14)$$

$\omega_r^L$ and $\omega_r^U$ meet the constraint,

$$\sum_{r=1}^{m} \omega_r^L(x) + \omega_r^U(x) = 1 \qquad (15)$$

and the value of $f\left(\omega_r^L(x), \omega_r^U(x)\right)$ is dependent on the type reduction methods and belongs to an interval. In this study, of minimax uncertainty bounds [40] is engaged for type reduction. Assigning $\left(\omega_r^L(x), \omega_r^U(x)\right)/2$ to $\left(\omega_r^L(x), \omega_r^U(x)\right)$ and substituting it into Eq. (21); leads to

$$u_k \in \left[u_k^{(O)}, u_k^{(M)}\right] \qquad (16)$$

Then, the uncertainty bounds can be calculated to be

$$\begin{cases} \overline{u}_{c,k} = \min\left\{u_k^{(O)}, u_k^{(M)}\right\} \\ \underline{u}_{c,k} = \overline{u}_{c,k} - \left[ \begin{array}{c} \dfrac{\sum_{i=1}^{m} \overline{\omega}^i - \underline{\omega}^i}{\sum_{i=1}^{m} \overline{\omega}^i \sum_{i=1}^{m} \underline{\omega}^i} \\ \times \dfrac{\sum_{i=1}^{m} \underline{\omega}^i (K_i - K_1)x \sum_{i=1}^{m} \overline{\omega}^i (K_m - K_i)x}{\sum_{i=1}^{m} \underline{\omega}^i (K_i - K_1)x + \sum_{i=1}^{m} \overline{\omega}^i (K_m - K_i)x} \end{array} \right] \end{cases} \qquad (17)$$

The lower bound $\underline{u}_{c,k}$ is designated to be equal to the upper bound $\overline{u}_{c,k}$ if only one rule is triggered (i.e., $m = 1$). The crisp output of the FLC is

$$\begin{cases} u_k \approx \dfrac{1}{2}\left(\underline{u}_{c,k} + \overline{u}_{c,k}\right) \\ \lambda_k = u_k \end{cases} \qquad (18)$$

For fairly comparative study, both the type-1 and type-2 MFs are designed by using widely-used triangle shapes, wherein their shapes are drawn following Ref. [39] and illustrated in Fig. 6.
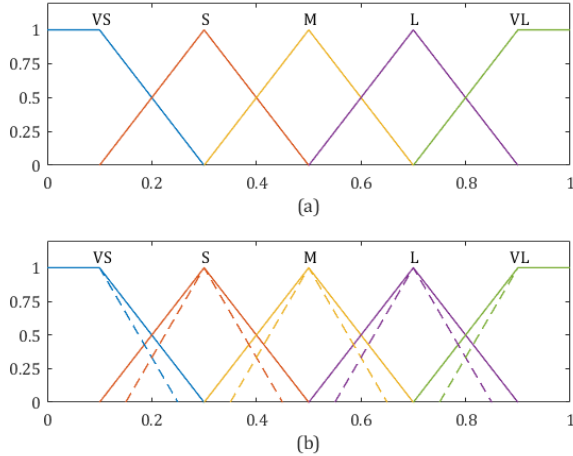


Fig. 6. MFs of the two input variables (i.e., $v_{avg}$ and $a_{rng}$): (a) type-1 MFs; (b) type-2 MFs

There are 25 fuzzy rules defined and used to infer an output of the style factor, as shown in Table II.

TABLE II
RULE BASE FOR $5 \times 5$ FUZZY LOGIC INFERENCE

| $v_{avg}$ | $a_{rng}$ | | | | |
|---|---|---|---|---|---|
| | VS | S | M | L | VL |
| VS | VG | VG | G | G | N |
| S | VG | G | G | N | A |
| M | G | G | N | A | A |
| L | G | N | A | A | VA |
| VL | N | A | A | VA | VA |

Finally, the optimized control parameters $\phi_\alpha$, $\phi_\beta$ were used to fit to the style factor $\lambda$ using the linear interpolation,

$$\phi = \phi_i + (\phi_{i+1} - \phi_i)\frac{\lambda - \lambda_i}{\lambda_{i+1} - \lambda_i}, \qquad \lambda \in [\lambda_i, \lambda_{i+1}] \quad (19)$$

where, index $i$ indicates the type of classified driving styles. Activated by Eq. (23), the proceed signal of driving style $\lambda$ can be calculated and used to adjust the inference rules of the SP strategy based on mapping relations between the style factor $\lambda$ and the control parameters $\phi_\alpha$, $\phi_\beta$.

## IV. TESTING AND VALIDATION SET-UP

### A. Driving Cycles

In this research, four typical laboratory driving cycles including Worldwide harmonized Light vehicle Test Cycle (WLTC), China Light-Duty Vehicle Test Cycle (CLTC), EPA Federal Test Cycle (FTP-75), and New European Driving Cycle (NEDC) are considered as the baseline to produce personalized driving cycles via the sub-driver model [36] by adjusting the style factor λ. For each laboratory driving cycle, five style-fixed and one style-free driving cycles (by adding a white noise signal to the style factor) are generated, namely, V. Gentle, Gentle, Normal, Aggressive, V. Aggressive.

TABLE III
DRIVING INFORMATION OF FOUR SUBJECTS

| Driver | Age | Time to hold a driving license (yrs.) | Annual mileage (mile) | Driving geography |
|---|---|---|---|---|
| A | 27 | 10 | 2000 | Urban |
| B | 24 | 7 | 2500 | Hybrid |
| C | 26 | 10 | 1500 | Hybrid |
| D | 26 | 4 | 6000 | Motorway |

In order to evaluate the vehicle system adaptability to real-world driving scenarios, personal driving cycles collected from our current research [38] have been adopted. There are four human drivers involved to produce real-time driving patterns (with a 10Hz sampling frequency) of 20-min driving signals via interacting with a driving simulator (supported by a Thrustmaster T500RS). With respect to real-world road conditions, the road map model used with reconstructed traffic simulates a cyclic undivided highway with uphill, downhill, curved and straight roads and is provided by IPG CarMaker. Table III organizes driving-related information about six subjects.

### B. Hardware in the loop Experiment

Hardware in the loop testing was carried out for the evaluation of the distributed system's real-time performance. It is used to shows an implementability that the driving style recognizer can work in distributed control layer. Meanwhile, all control variables in the energy management system need to be solved in real time at the same time step in order to restore the real controller's calculation mechanism as much as possible. This research adopts the industry standard experimental facilities supplied by the ETAS Group. The framework of the HiL experimental platform is shown in Fig. 6.

The distributed computing and V2I communication were performed by an ETAS ES910 and its basic components are a 1.5GHz microprocessor with 4GB RAM and 1Gbps Ethernet communication. The function of driving style recognition was

encoded into host PC-1 and flashed to the ES910 by ETAS INTECRIO. The DESKLABCAR functions as the PHEV with the local controller and communicates with the V2I interface (ES910) through a CAN bus. Models of the vehicle and the local controller were compiled in host PC-2 and downloaded to the DESK-LABCAR by the ETAS experimental environment via Ethernet protocol. In this study, the sampling time is 10 Hz and the vehicle performance is governed by the ETAS experimental environment in host PC-2. Thanks to the rule-based SP control strategy, we found that there was still a surplus of computing resources in the experimental platform.
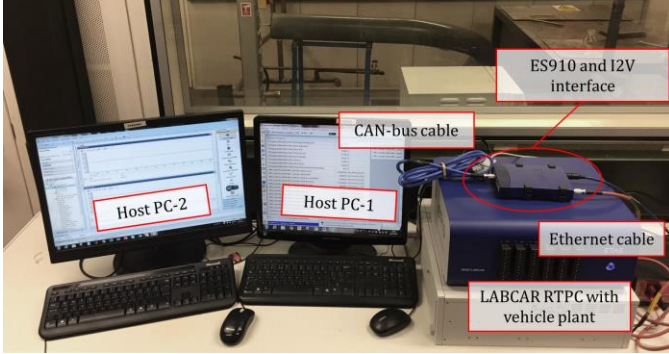


Fig. 7. Hardware-in-the-loop experimental platform

## V. RESULTS AND DISCUSSION

### A. Pareto Analysis and Energy-saving Performance

Before discussing the distributed cooperative EMS, the SP control strategies with the proposed personalized non-stationary inference used in the on-board controller needs to be verified first. This section studies influence of the weighting factor and diverse driving styles on energy-saving performance. The targeting five driving cycles has 400km driving length which is composed of four laboratory cycles i.e., CLTC, WLTC, FTP-75, and NEDC, wherein each laboratory cycle is reproduced with five driving styles and extended to 100km. For fair comparison, the optimal control parameters of each case are obtained by using CAPSO algorithm with the same 100 iterations.
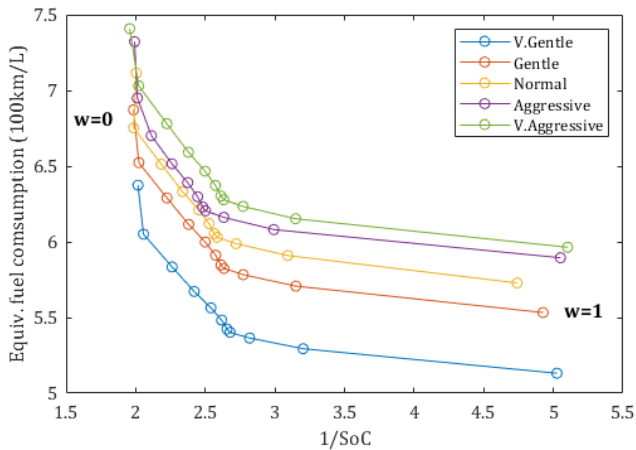


Fig. 8. Pareto Frontier for different settings of the weight factor

Here, a Pareto analysis is performed as illustrated in Fig. 8 to investigate the influence of the weight value $w$ on the trade-off between minimizing the total used energy and maximizing the BP's SoC. The weight value $w \in [0,1]$ determines the preference of the objectives, namely, when $w = 0$, the CAPSO algorithm only seeks to minimize the total used energy, similarly, when $w = 1$, it only seeks to maximize the BP's SoC. As can be seen, the total energy decreased by allowing the BP's SoC to decrease from the most effective configuration, in which the reducing rate of the total energy is continuously decreasing. To reflect an equal preference towards relatively lower energy consumption with a safe level of SoC, the weight value is set here to a fixed value of 0.7 as considered in [32].

TABLE IV
OVERALL PERFORMANCE COMPARISON OF USING
DIFFERENT CONTROL STRATEGIES OVER COMBINED FOUR
LABORATORY DRIVING CYCLES

| Driving style | Control strategy | Final SoC | Equiv. fuel consumption (100km/L) | Savings (%) |
|---|---|---|---|---|
| Very Gentle | SP-SI | 0.402 | 5.872 | |
| | ECMS | 0.245 | 5.564 | 5.25% |
| | SP-PNSI | 0.370 | 5.402 | 8.00% |
| Gentle | SP-SI | 0.393 | 6.185 | |
| | ECMS | 0.230 | 5.999 | 3.01% |
| | SP-PNSI | 0.381 | 5.824 | 5.84% |
| Normal | SP-SI | 0.401 | 6.290 | |
| | ECMS | 0.231 | 6.170 | 1.91% |
| | SP-PNSI | 0.399 | 5.980 | 4.93% |
| Aggressive | SP-SI | 0.414 | 6.415 | |
| | ECMS | 0.235 | 6.331 | 1.31% |
| | SP-PNSI | 0.402 | 6.205 | 3.27% |
| Very Aggressive | SP-SI | 0.399 | 6.492 | |
| | ECMS | 0.229 | 6.466 | 0.40% |
| | SP-PNSI | 0.384 | 6.278 | 3.30% |

Table IV compares energy-saving performance of three control strategies used in the studied vehicle system for each driving style. They are the SP control strategies with stationary inference (i.e., SP-SI) and the proposed personalized non-stationary inference (i.e., SP-PNSI), and the equivalent consumption minimization strategy (ECMS). Evidently, the vehicle system using the proposed SP-PNSI strategy outperforms the system using ECMS or SP-SI strategy for different driving styles. There is an approximately linear relationship between the equivalent fuel consumption and aggressiveness of driving style, but the trending of rises is reduced gradually. It appears that too mild actions signify lower power demand so that the control strategy has greater latitude in optimizing between the different traction modes. By using the combined laboratory cycles in Very Gentle style, the results show the proposed SP-PNSI strategy has a significant reduction in equivalent fuel consumption (L/100 km) of 8.00% from the SP-PNSI one, compared to 5.25% reduction by using the ECMS.

Fig. 9(a) further investigate impact of using different control strategies on energy-saving performance for each studied laboratory driving cycle during Normal in driving style. Overall, the proposed SP-PNSI strategy performs the lowest equivalent fuel consumption compared other two in all four cases (at least 0.66% of reduction, compared to ECMS). From a view of laboratory cycles, using the latest released CLTC as a target cycle for control optimization has the highest equivalent

fuel consumption in studied four (up to 8.70% of rises compared to using NEDC). Over time, not only the emission regulations have become stricter, but the aggressiveness degree of driving patterns in the laboratory cycle has also increased significantly. Fig. 9(b) illustrates the engine operation map during the WLTC with Normal driving style, in which the color bar represents the corresponding thermal efficiency (%) of the ICE. The initial SoC value is set to 50% in order to focus on the conversion of multiple energy sources in CD/CS mode. It can be seen from the highlighted equivalent operating points (black dotted circle) that using the proposed SP-PNSI strategy leads to more operating points of the engine in the high-efficiency area (marked in yellow) compared to the ECMS and SP-SI strategy.
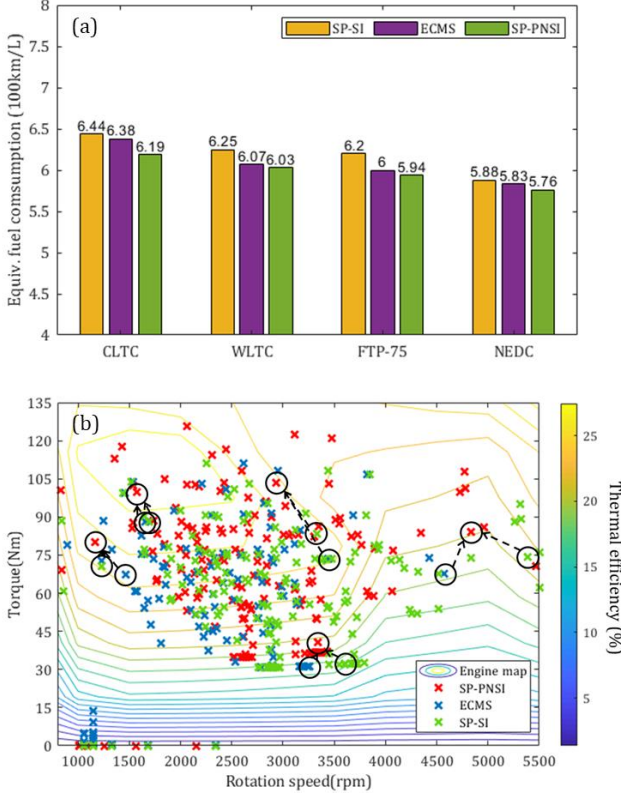


Fig. 9. Energy-saving performance comparison of using different control strategies during Normal in driving style: a) over four laboratory driving cycles; and b) Engine operation map over WLTC

### B. Vehicle System Adaptability to Human Drivers

To evaluate adaptability of the distributed cooperative EMS, HiL testing was conducted under real-time driving scenarios with four personal driving cycles (extend to 100km per each). The commonly used threshold-based driving style recognition algorithm with equalized classification has been involved as a control group to compare with the fuzzy-based them.

Fig. 10 shows real-time performance of velocity and style recognition for four human drivers at the first 1200 s. Compared to threshold-based recognition algorithm, two fuzzy based they perform the smoother recognition signals with less overshooting. In Fig. 10(a), threshold-based recognition algorithm offers the signal with Very Aggressive in style when the vehicle velocity fluctuates greatly, but two fuzzy based they offer the signal with Aggressive in style. Fig. 11 illustrates driving aggressiveness distribution in 100 km for each driver by using three driving recognition algorithms. Compared to type-

1 and type-2 fuzzy based recognition algorithms, threshold-based one is impossible to have a chance for a signal response with Very Gentle. This means that the threshold-based recognition algorithm lacks diversity in driving aggressiveness quantification. Relatively, the expression of type-1 and type-2 fuzzy based are more precise and extensive.
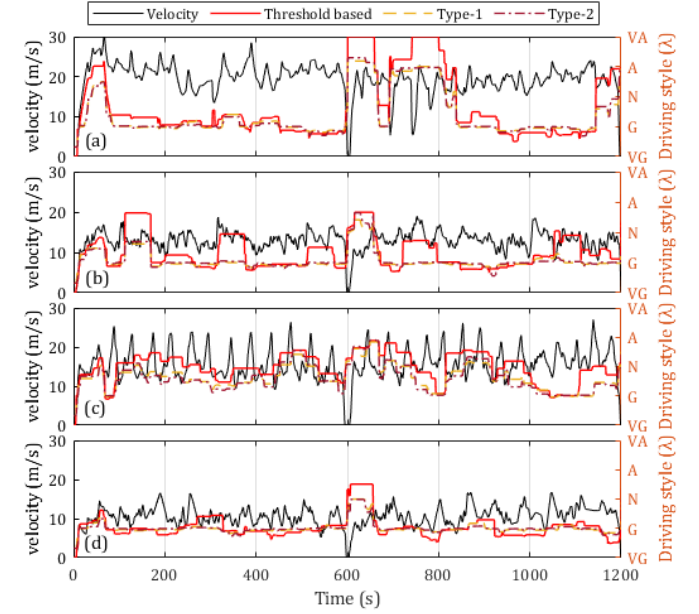


Fig. 10. Real-time performance of driving style recognition performance by using three driving recognition algorithms for: a) Driver A; b) Driver B; c) Driver C; and d) Driver D
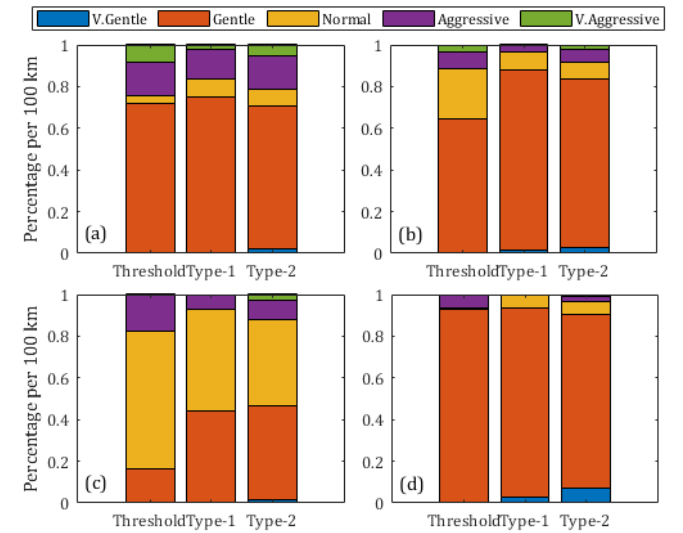


Fig. 11. Driving aggressiveness distribution (per 100 km) by using different algorithms for: a) Driver A; b) Driver B; c) Driver C; and d) Driver D

On the performance of energy consumption, Table V summarizes equivalent fuel consumption of the proposed distributed cooperative EMSs by using the studied three style recognition algorithms. From a view of driver identity, Driver C with more aggressive driving style has the worst equivalent fuel consumption (6.94 L/100km) rather than other drivers have. Driver D is the most moderate one (6.43 L/100km). From a view of recognition algorithm, type-2 fuzzy based recognition algorithm shows superior energy-saving performance with up to 2.64% reduction in equivalent fuel consumption compared to

other two algorithms. Because of optimization results based on laboratory cycles, vehicle system performance to human drivers has a certain degree of deterioration in equivalent fuel consumption but the proposed distributed cooperative EMSs by using type-2 fuzzy based recognition algorithm has the lowest affect.

TABLE V
ENERGY CONSUMPTION (L/100 KM) COMPARISON OF USING DIFFERENT DRIVING STYLE RECOGNITION ALGORITHMS

| Algorithm | Driver A | Driver B | Driver C | Driver D | Averaged |
|---|---|---|---|---|---|
| Threshold | 6.93 | 6.74 | 7.14 | 6.48 | 6.82 |
| Type-1 | 6.88 | 6.62 | 6.90 | 6.44 | 6.71 |
| Type-2 | 6.81 | 6.56 | 6.79 | 6.38 | 6.64 |
| Averaged | 6.87 | 6.64 | 6.94 | 6.43 | 6.72 |

### C. Effect of Communication Quality

Efficient communication is the key to the success of the distributed system. However, signal loss and delay also happen from time to time. For distributed EMSs, the quality of the signal sent and received by the vehicle terminal as a whole has to be seriously considered. In view of this, this section discusses the impact of signal loss and delay on the distributed cooperative EMS, respectively. To emulate signal loss of the V2X network between the vehicle and roadside unit, six levels of signal loss rate are considered and were used to investigate the robustness of the proposed distributed cooperative EMS. A trigger square signal was designed to multiply the original signal, where each trigger segment is used to activate the function of driving style recognition and its duration is fixed at 30 s. Conversely, the non-trigger segment is used to deactivate the function of driving style recognition and its duration is based on the signal loss rate.
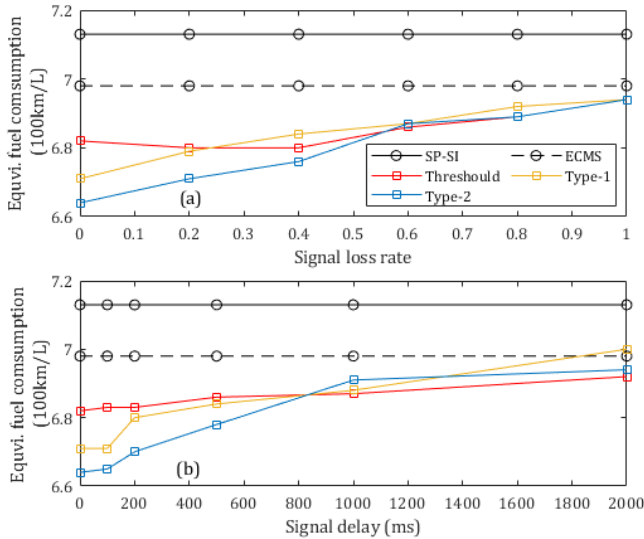


Fig. 12. System robustness performance under different degrees of: (a) signal loss and (b) delay

From the result, the ECMS and the SP-SI strategy are not affected by signal loss because their control policies do not need to be updated during real-time driving. As signal loss rate increases, the energy consumption of the distributed cooperative EMSs using type-1 and type-2 fuzzy based style recognizers both increase gradually. When the signal is completely lost, their performance is still higher than that obtained by using the ECMS (1.11%) and the conventional SP-

SI strategy (4.31%). Therefore, the proposed the distributed cooperative EMSs can improve fuel economy even under harsh communication conditions, especially when applying type-2 fuzzy based style recognizer. According to [30], 0-2000 ms is a regular range of latency of DSRC and 4G-LTE for connected vehicles. Fig. 12(b) investigates the impact of signal latency on equivalent fuel consumption of the proposed distributed cooperative EMS. The energy consumption of the distributed cooperative EMSs using type-1 and type-2 fuzzy based style recognizers are significantly affected by the signal delay, compared to that using threshold-based style recognizer. Under the condition of 2000ms delay, the energy consumption of using type-1 based style recognizer is not even as good as ECMS.

TABLE VI
EQUIVALENT FUEL CONSUMPTION (L/100 KM) COMPARISON OF THE PROPOSED DISTRIBUTED COOPERATIVE EMS UNDER DIFFERENT DEGREES OF SIGNAL LOSS AND DELAY

| Signal delay (ms) | Signal loss (%) | | | | | | |
|---|---|---|---|---|---|---|---|
| | 0 | 20 | 40 | 60 | 80 | 100 | Overall |
| 0 | 6.64 | 6.71 | 6.76 | 6.87 | 6.89 | 6.94 | 6.80 |
| 100 | 6.65 | 6.72 | 6.75 | 6.82 | 6.90 | 6.94 | 6.80 |
| 200 | 6.7 | 6.72 | 6.77 | 6.86 | 6.88 | 6.94 | 6.81 |
| 500 | 6.78 | 6.84 | 6.87 | 6.89 | 6.93 | 6.94 | 6.88 |
| 1000 | 6.91 | 6.94 | 6.92 | 6.92 | 6.96 | 6.94 | 6.93 |
| 2000 | 6.94 | 6.91 | 6.92 | 6.95 | 6.93 | 6.94 | 6.93 |
| Overall | 6.77 | 6.81 | 6.83 | 6.89 | 6.91 | 6.94 | 6.86 |

Table VI summaries equivalent fuel consumption of the proposed distributed cooperative EMS (Type-2) under different degrees of signal loss and delay. From a view of signal delay, 200-1000 ms is the most sensitive interval of equivalent fuel consumption. Under the dual effects of signal loss and delay, the highest equivalent fuel consumption (6.96 L/100km) occurs at points with 1000 ms of delay and 80% of signal loss, even over those when signals fully loss (6.94 L/100km). When network signal delay is detected (>1000 ms), deactivating the function of driving style recognition may be an alternative way to ensure the vehicle system robustness. Through the comprehensive study, the proposed distributed cooperative EMS has a great potential to apply in cyber-physical system of connected vehicles in the near future. With less onboard computational burden and communication, the proposed system is expected to save more energy for PHEVs in practice.

### V. CONCLUSION

This paper developed a distributed cooperative EMS for connected plug-in hybrid electric vehicles. By introducing personalized non-stationary inference, this system can fuse driving behavior and vehicle state information to adaptively adjust power-split control parameters for vehicle energy economy improvement. Through HiL testing, the proposed distributed cooperative EMS has an ability to adapt well to differing driving styles, even when there is signal loss and delay. The conclusions drawn from the investigation are as follows:

1) Compared to the conventional SP strategy, up to 8% energy can be saved over WLTC by using a SP strategy with personalized non-stationary inference, especially for very gentle drivers.

2) Over the studied four personal driving cycles, generally, the driving style recognizer driven by type-2 fuzzy sets helps save 1.04% of energy compared to that driven by type-1 fuzzy sets and save 2.64% of energy compared to that driven by threshold-based recognizer.

3) In the survey scope of signal delay 0 - 2000 ms, signal delays of 200 ms and 1000 ms have the most sensitive scope on the energy consumption of the proposed system. Compared to no delay condition, an increase of equivalent fuel consumption varies from 0.14% to 1.91%.

4) When the control signal is completely lost, energy-saving performance of the improved vehicle system is still higher than that of the ECMS (by 0.57%) and the conventional SP strategy (by 2.66%).

Three main contributions to be made from the investigation are: 1) the framework of the distributed cooperative EMS is designed to fuse driving behaviors and vehicle state information to adapt to various changes of driving behaviors for improving vehicle energy economy; 2) for personalizing the conventional stationary inference rule, chaos-enhanced accelerated particle swarm optimization is tailored with an additional nest for different driving behaviors to obtain the optimal power-split control parameters over the combined laboratory cycle; and 3) a driving style recognizer with type-2 fuzzy sets is developed to monitor driving behaviors in real-time and maintain the system robustness under different degrees of signal delay and loss.

## REFERENCES

[1] I. Mukerjee, "UK TRANSPORT VISION 2050: investing in the future of mobility," *Innovate UK*, no. August, 2021.

[2] European Commission, "Roadmap 2050 - Technical & Economic Analysis - Full Report," *Publications Office of the European Union*, pp. 1–100, 2016.

[3] T. Liu, W. Tan, X. Tang, J. Zhang, Y. Xing, and D. Cao, "Driving conditions-driven energy management strategies for hybrid electric vehicles: A review," *Renew. Sustain. Energy Rev.*, vol. 151, no. July, p. 111521, 2021, doi: 10.1016/j.rser.2021.111521.

[4] J. Li, Q. Zhou, H. Williams, H. Xu, and C. Du, "Cyber-Physical Data Fusion in Surrogate-assisted Strength Pareto Evolutionary Algorithm for PHEV Energy Management Optimization," *IEEE Trans. Ind. Informatics*, 2021.

[5] D. D. Tran, M. Vafaeipour, M. El Baghdadi, R. Barrero, J. Van Mierlo, and O. Hegazy, "Thorough state-of-the-art analysis of electric and hybrid vehicle powertrains: Topologies and integrated energy management strategies," *Renew. Sustain. Energy Rev.*, vol. 119, p. 109596, 2020, doi: 10.1016/j.rser.2019.109596.

[6] W. Shabbir and S. A. Evangelou, "Threshold-changing control strategy for series hybrid electric vehicles," *Appl. Energy*, vol. 235, no. November 2018, pp. 761–775, 2019, doi: 10.1016/j.apenergy.2018.11.003.

[7] Q. Zhou, D. Zhao, B. Shuai, Y. Li, H. Williams, and H. Xu, "Knowledge Implementation and Transfer With an Adaptive Learning Network for Real-Time Power Management of the Plug-in Vehicle," *IEEE Trans. Neural Networks Learn. Syst.*, vol. PP, pp. 1–11, 2021, doi: 10.1109/TNNLS.2021.3093429.

[8] Q. Zhou *et al.*, "Transferable Representation Modelling for Real-time Energy Management of the Plug-in Hybrid Vehicle based on K-fold Fuzzy Learning and Gaussian Process Regression," *Appl. Energy*, 2021.

[9] G. Paganelli, S. Delprat, T. M. Guerra, J. Rimaux, and J. J. Santin, "Equivalent consumption minimization strategy for parallel hybrid powertrains," *IEEE Veh. Technol. Conf.*, vol. 4, no. May 2014, pp. 2076–2081, 2002, doi: 10.1109/VTC.2002.1002989.

[10] S. Yang, J. Wang, F. Zhang, and J. Xi, "Self-Adaptive Equivalent Consumption Minimization Strategy for Hybrid Electric Vehicles," *IEEE Trans. Veh. Technol.*, vol. 70, no. 3, pp. 2124–2137, 2021, doi: 10.1109/TVT.2021.3059205.

[11] R. Bellman, "Dynamic Programming," *Science (80-. ).*, vol. 153, no. 3731, pp. 34–37, 1966.

[12] J. Peng, H. He, and R. Xiong, "Rule based energy management strategy for a series – parallel plug-in hybrid electric bus optimized by dynamic programming," *Appl. Energy*, vol. 185, pp. 1633–1643, 2017, doi: 10.1016/j.apenergy.2015.12.031.

[13] G. Li and D. Gorges, "Fuel-Efficient Gear Shift and Power Split Strategy for Parallel HEVs Based on Heuristic Dynamic Programming and Neural Networks," *IEEE Trans. Veh. Technol.*, vol. 68, no. 10, pp. 9519–9528, 2019, doi: 10.1109/TVT.2019.2927751.

[14] C. M. Martinez, M. Heucke, F. Wang, B. Gao, and D. Cao, "Driving Style Recognition for Intelligent Vehicle Control and Advanced Driver Assistance : A Survey," *IEEE Trans. Intell. Transp. Syst.*, vol. 19, no. 3, pp. 666–676, 2018, doi: 10.1109/TITS.2017.2706978.

[15] V. Manzoni, A. Corti, P. De Luca, and S. M. Savaresi, "Driving style estimation via inertial measurements," *IEEE Conf. Intell. Transp. Syst. Proceedings, ITSC*, pp. 777–782, 2010, doi: 10.1109/ITSC.2010.5625113.

[16] A. Corti, C. Ongini, M. Tanelli, and S. M. Savaresi, "Quantitative driving style estimation for energy-oriented applications in road vehicles," *Proc. - 2013 IEEE Int. Conf. Syst. Man, Cybern. SMC 2013*, pp. 3710–3715, 2013, doi: 10.1109/SMC.2013.632.

[17] F. U. Syed, D. Filev, and H. Ying, "Fuzzy rule-based driver advisory system for fuel economy improvement in a hybrid electric vehicle," *Annu. Conf. North Am. Fuzzy Inf. Process. Soc. - NAFIPS*, pp. 178–183, 2007, doi: 10.1109/NAFIPS.2007.383833.

[18] B. C. Miyajima *et al.*, "Driver Modeling Based on Driving Behavior and Its Evaluation in Driver Identification," 2007.

[19] D. Ding, Q. L. Han, Z. Wang, and X. Ge, "A Survey on Model-Based Distributed Control and Filtering for Industrial Cyber-Physical Systems," *IEEE Trans. Ind. Informatics*, vol. 15, no. 5, pp. 2483–2499, 2019, doi: 10.1109/TII.2019.2905295.

[20] V. Nikam and V. Kalkhambkar, "A review on control strategies for microgrids with distributed energy resources, energy storage systems, and electric vehicles," *Int. Trans. Electr. Energy Syst.*, vol. 31, no. 1, pp. 1–26, 2021, doi: 10.1002/2050-7038.12607.

[21] W. Tushar *et al.*, "Peer-to-peer energy systems for connected communities: A review of recent advances and emerging challenges," *Appl. Energy*, vol. 282, no. PA, p. 116131, 2021, doi: 10.1016/j.apenergy.2020.116131.

[22] P. Duan, H. Soleimani, A. Ghazanfari, and M. Dehghani, "Distributed Energy Management in Smart Grids Based on Cloud-Fog Layer Architecture Considering PHEVs," *IEEE Trans. Ind. Appl.*, vol. 9994, no. c, pp. 1–1, 2020, doi: 10.1109/tia.2020.3010899.

[23] J. Li *et al.*, "Pedestrian-Aware Supervisory Control System Interactive Optimization of Connected Hybrid Electric Vehicles via Fuzzy Adaptive Cost Map and Bees Algorithm," *IEEE Trans. Transp. Electrif.*, vol. 7782, no. c, pp. 1–1, 2021, doi: 10.1109/tte.2021.3124606.

[24] X. Hu, H. Wang, and X. Tang, "Cyber-Physical Control for Energy-Saving Vehicle Following with Connectivity," *IEEE Trans. Ind. Electron.*, vol. 64, no. 11, pp. 8578–8587, 2017, doi: 10.1109/TIE.2017.2703673.

[25] K. Lin, C. Li, Y. Li, C. Savaglio, and G. Fortino, "Distributed Learning for Vehicle Routing Decision in Software Defined Internet of Vehicles," *IEEE Trans. Intell. Transp. Syst.*, vol. 22, no. 6, pp. 3730–3741, 2021, doi: 10.1109/TITS.2020.3023958.

[26] S. E. Li and Y. Zheng, "Dynamical Modeling and Distributed Control of Connected and Automated Vehicles: Challenges and Opportunities," *IEEE Intell. Transp. Syst. Mag.*, vol. 9, pp. 46–58, 2017.

[27] Q. Zhou *et al.*, "Multi-step Reinforcement Learning for Model-Free Predictive Energy Management of an Electrified Off-highway Vehicle," *Appl. Energy*, vol. 255, no. 2019, pp. 588–601, 2019.

[28] J. Li *et al.*, "Dual-loop online intelligent programming for driver-oriented predict energy management of plug-in hybrid electric vehicles," *Appl. Energy*, vol. 253, no. November, p. 113617, 2019, doi: 10.1016/j.apenergy.2019.113617.

[29] Z. Xu, X. Li, X. Zhao, M. H. Zhang, and Z. Wang, "DSRC versus 4G-LTE for connected vehicle applications: A study on field experiments of vehicular communication performance," *J. Adv. Transp.*, vol. 2017, 2017, doi: 10.1155/2017/2750452.

[30] K. C. Dey, A. Rayamajhi, M. Chowdhury, P. Bhavsar, and J. Martin, "Vehicle-to-vehicle (V2V) and vehicle-to-infrastructure (V2I)

communication in a heterogeneous wireless network - Performance evaluation," *Transp. Res. Part C Emerg. Technol.*, vol. 68, pp. 168–184, 2016, doi: 10.1016/j.trc.2016.03.008.

[31] M. Ehsani, Y. Gao, S. Longo, and K. Ebrahimi, *Modern electric, hybrid electric, and fuel cell vehicles*. CRC press, 2018.

[32] J. Li, Q. Zhou, H. Williams, and H. Xu, "Back-to-back competitive learning mechanism for fuzzy logic based supervisory control system of hybrid electric vehicles," *IEEE Trans. Ind. Electron.*, vol. 67, no. 10, pp. 8900–8909, 2020, doi: 10.1109/TIE.2019.2946571.

[33] Q. Zhou, Y. Zhang, Z. Li, J. Li, H. Xu, and O. Olatunbosun, "Cyber-Physical Energy-Saving Control for Hybrid Aircraft-Towing Tractor Based on Online Swarm Intelligent Programming," *IEEE Trans. Ind. INFORMATICS*, vol. 14, no. 9, pp. 4149–4158, 2018, doi: 10.1109/TII.2017.2781230.

[34] Z. Chen, R. Xiong, C. Wang, and J. Cao, "An on-line predictive energy management strategy for plug-in hybrid electric vehicles to counter the uncertain prediction of the driving cycle," *Appl. Energy*, vol. 185, pp. 1663–1672, 2017, doi: 10.1016/j.apenergy.2016.01.071.

[35] Y. Zhang *et al.*, "Optimal energy management strategy for parallel plug-in hybrid electric vehicle based on driving behavior analysis and real time traffic information prediction," *Mechatronics*, vol. 46, pp. 177–192, 2017, doi: 10.1016/j.mechatronics.2017.08.008.

[36] J. Kennedy, "Particle swarm optimization," in *Encyclopedia of machine learning*, Springer, pp. 760–766.

[37] A. H. Gandomi, G. J. Yun, X. S. Yang, and S. Talatahari, "Chaos-enhanced accelerated particle swarm optimization," *Commun. Nonlinear Sci. Numer. Simul.*, vol. 18, no. 2, pp. 327–340, 2013, doi: 10.1016/j.cnsns.2012.07.017.

[38] J. Li, Q. Zhou, Y. He, H. Williams, and H. Xu, "Driver-identified Supervisory Control System of Hybrid Electric Vehicles based on Spectrum-guided Fuzzy Feature Extraction," *IEEE Trans. Fuzzy Syst.*, vol. 6706, no. c, pp. 1–1, 2020, doi: 10.1109/tfuzz.2020.2972843.

[39] J. Cao, P. Li, and H. Liu, "An Interval Fuzzy Controller for Vehicle Active Suspension Systems," *IEEE Trans. Intell. Transp. Syst.*, vol. 11, no. 4, pp. 885–895, 2010, doi: 10.1109/TITS.2010.2053358.

[40] J. M. Mendel, "Advances in type-2 fuzzy sets and systems," *Inf. Sci. (Ny).*, vol. 177, no. 1, pp. 84–110, 2007, doi: 10.1016/j.ins.2006.05.003.

**Ji Li** (M'19) awarded the Ph.D. degree in mechanical engineering from the University of Birmingham, U.K, in 2020. He is currently a Research Fellow and works on the Connected and Autonomous Systems for Electrified Vehicles at the Vehicle Technology Research Centre. His current research interests include computational intelligence, informatic fusion, data-driven modelling, man-machine system, and their applications on connected and autonomous vehicles.

**Quan Zhou** (M'17) received the Ph.D. degree in mechanical engineering from the University of Birmingham in 2019 that was distinguished by being the school's solo recipient of the University of Birmingham's Ratcliffe Prize of the year. He is currently a Research Fellow and leads the Connected and Autonomous Systems for Electrified Vehicles Research at University of Birmingham. His research interests include evolutionary computation, fuzzy logic, reinforcement learning, and their application in vehicular systems.

**Yinglong He** received the Ph.D. degree in mechanical engineering from the University of Birmingham, UK, in 2021. He is currently working with the European Commission Joint Research Centre. His main research interests include connected, automated, and electrified vehicles, intelligent transportation systems, advanced driver-assistance systems, multi-objective optimization, and machine learning.

**Huw Williams** received the B.A. and M.A. degrees in mathematics from the University of Oxford, Oxford, U.K., in 1978 and 1983, respectively, and the Ph.D. degree in theoretical mechanics from the University of East Anglia, Norwich, U.K. He is an Honorary Professor of Energy and Automotive Engineering at the UoB, Birmingham, U.K. He is a professional mathematician with excellent skills in Lean, Six Sigma, Engineering Physics and Statistics. Huw has over 20 years' experience in the automotive industry. He also developed statistical skills through TQM in the 1980's culminating in his accreditation as Ford's top-scoring Master Black Belt in 2005.

**Hongming Xu** received the Ph.D. degree in mechanical engineering from Imperial College London, London, U.K., in 1995. He is a Professor of Energy and Automotive Engineering at the University of Birmingham, Birmingham, U.K., and Head of Vehicle and Engine Technology Research Centre. He has six years of industrial experience with Jaguar Land Rover. He has authored and co-authored more than 400 journal and conference publications on advanced vehicle powertrain systems involving both experimental and modeling studies.

**Guoxiang Lu** received the Ph.D. degree in control engineering from South China University of Technology, China, in 2010. He started a research fellow and led the development of modern engine control at the UoB, U.K., in 2015. He is currently senior manager at department of research and development of renewable and sustainable vehicles, BYD Auto Ltd, Guangzhou, China. His research interests include GDI engine combustion control, system modeling, real-time control, engine control strategy development, and intelligent vehicle system.